Correlation between *in Vitro* Stability and *in Vivo* Performance of Anti-GCN4 Intrabodies as Cytoplasmic Inhibitors*

Arne Wörn‡, Adrian Auf der Maur§, Dominik Escher§¶, Annemarie Honegger‡, Alcide Barberis§¶, and Andreas Plückthun‡‖

From the ‡Biochemisches Institut, §ESBATech Inc., ¶Institut für Molekularbiologie, Universität Zürich, Winterthurerstrasse 190, CH-8057 Zürich, Switzerland

A cellular assay system for measuring the activity of cytoplasmically expressed anti-GCN4 scFv fragments directed against the Gcn4p dimerization domain was established in the budding yeast *Saccharomyces cerevisiae*. The inhibitory potential of different constitutively expressed anti-GCN4 scFv intrabodies was monitored by measuring the activity of β-galactosidase expressed from a *GCN4*-dependent reporter gene. The *in vivo* performance of these scFv intrabodies in specifically decreasing reporter gene activity was related to their *in vitro* stability, measured by denaturant-induced equilibrium unfolding. A framework-engineered stabilized version showed significantly improved activity, while a destabilized point mutant of the anti-GCN4 wild-type showed decreased effects *in vivo*. These results indicate that stability engineering can result in improved performance of scFv fragments as intrabodies. Increasing the thermodynamic stability appears to be an essential factor for improving the yield of functional scFv in the reducing environment of the cytoplasm, where the conserved intradomain disulfides of antibody fragments cannot form.

Antibodies are secreted by plasma cells and have evolved to act in a variety of compartments of the mammalian body outside of cells. The demands on stability have kept a selection pressure on immunoglobulin domains to retain disulfide bonds in all germline genes. The disulfide bonds form during the process of secretion in the endoplasmic reticulum. Over the last decade, a wide variety of recombinant antibody formats has been engineered, such as *e.g.* the single-chain Fv (scFv)[1] fragment (1, 2), which consists only of the variable domains connected by a linker. These different antibody fragments can be produced in a series of different hosts, ranging from bacteria to mammalian cells, usually by still exploiting disulfide formation in the host secretion pathway. However, it is also possible to express scFv or Fab fragments within eukaryotic and bacterial cells in functional form, at least to some level (3–6). A sufficient functional expression, *i.e.* correct folding, of such intracellular antibodies (intrabodies), would enable them to bind to their target protein and evoke specific biological effects.

Assuming that this problem can be solved, intrabodies have been discussed as having great potential in functional genomics as the "protein equivalent" of antisense RNA. In the long term, intrabodies may even find broad therapeutic applications, possibly in a gene therapy setting (5). For example, by first transferring the cDNA encoding a specific intrabody fragment, directed against a viral regulatory protein, into a cell population by an *ex vivo* gene transfer, and second, reimplanting these cells into the patient, these cells would be made "immune" against infection or propagation of the particular virus.

In principle, intrabodies can be directed to all intracellular compartments by encoding the corresponding signal sequence attached to the antibody fragment (4, 5). Among these different intracellular locations, expression in the cytoplasm is the most difficult task, because of its reducing environment (7). This reducing potential prevents the formation of disulfide bonds, including the conserved intradomain disulfides in antibody domains (see Refs. 8 and 9 and references therein). Indeed, it was found that scFv fragments expressed cytoplasmically in COS cells do not form the disulfide bonds (10). The intradomain disulfide contributes about 4–5 kcal/mol to the stability of antibody domains (11, 12). Therefore, antibody fragments expressed in a reducing environment are strongly destabilized, compared with the same molecules containing disulfides, and a smaller fraction of these fragments is likely to fold to the correct native structure. This fact is believed to be responsible for the frequently observed reduced functional expression level of cytoplasmically expressed antibody fragments, as well as for their high tendency to form aggregates (10, 13).

Nevertheless, a number of cytoplasmically expressed antibody fragments were reported to show specific biological effects (see Refs. 14–16 for representative examples). However, for many applications the observed effects are insufficient, and such intrabodies would require further optimization by protein engineering. Moreover, if this technology is to be applied in a high-throughput fashion in functional genomics, a reliable access to these molecules is needed, and an investigation of the limiting factor is therefore required.

A class of proteins which constitute suitable targets for cytoplasmically expressed antibody fragments are transcriptional activators. Their functional inhibition by a specific intrabody can result in reduced transcription of the target gene

---

‖ To whom correspondence should be addressed: Biochemisches Institut, Universität Zürich, Winterthurerstrasse 190, 8057 Zürich, Switzerland. Tel.: 41-1-635-5570; Fax: 41-1-635-5712; E-mail: plueckthun @biocfebs.unizh.ch.

[1] The abbreviations used are: scFv, antibody single-chain Fv fragment; CDR, complementarity determining region; COS cells, SV40 transformed kidney cell line of *Cercopithecus aethiops*; Fab, antigen-binding fragment of an antibody; GdnHCl, guanidinium hydrochloride; Ig, immunoglobulin; K_D, equilibrium dissociation constant; p185HER2, extracellular domain of human epidermal growth factor receptor; SPR, surface plasmon resonance; V_H, variable domain of the heavy chain; V_L, variable domain of the light chain; BSA, bovine serum albumin; PCR, polymerase chain reaction; ELISA, enzyme-linked immunosorbent assay.

products, controlled by this specific transcriptional activator. The scFv fragment derived from an anti-p21[ras] antibody expressed in *Xenopus laevis*, for example, colocalized with the endogenous p21[ras] protein and inhibited p21[ras]-dependent H1-kinase activity induced by insulin (17). In another experiment, expression of the DO-1 scFv, directed against an N-terminal epitope of p53, reduced the activity of a p53-dependent reporter gene by about 50% (18).

The present study uses endogenous Gcn4p of the budding yeast *Saccharomyces cerevisiae* as a target protein for cytoplasmically expressed scFv fragments. Gcn4p belongs to the family of transcriptional activators with a leucine zipper motif (19) and binds as a homodimer to the sequence ATGA(C/G)TCAT (20). Its expression is controlled at the translational level and increases under conditions of amino acid starvation (21). In wild-type yeast, Gcn4p activates the transcription of many genes which encode enzymes involved in amino acid synthesis (22). To monitor Gcn4p activity, a *lacZ* reporter gene was placed under the control of *GCN4*. This system was used to investigate the correlation between *in vitro* stability (measured by denaturant-induced equilibrium unfolding of the purified scFv fragment), antigen affinity, and *in vivo* inhibition of Gcn4p by the cytoplasmically expressed anti-GCN4 scFv fragments.

EXPERIMENTAL PROCEDURES
ScFv Fragments Cytoplasmically Expressed in Yeast

The anti-GCN4 wild-type scFv has originally been obtained by ribosome display from a library constructed from an immunized mouse (23). The antigen was a double proline mutant of the Gcn4p leucine zipper, called 7P14P (indicating that positions 7 and 14 of the zipper domain are mutated to Pro residues), which forms a random coil in solution (24). The scFv fragment prevents dimerization of the wild-type Gcn4p coiled coil peptide *in vitro* (25), as it also binds the wild-type peptide as a monomer in a random coil conformation. The anti-GCN4 scFv fragment referred to as "wild-type" in the present study has been measured to have a dissociation constant of $4 \cdot 10^{-11}$ M from the leucine zipper peptide (23).

In the present study, several different mutants of this scFv were investigated. Besides the anti-GCN4 wild-type, a destabilized variant of the anti-GCN4 wild-type, which carries the heavy chain mutation Arg(H66) to Lys (termed anti-GCN4(H-R66K)), served as an example for a Gcn4p binding scFv fragment with essentially identical antigen binding properties, but with slightly decreased *in vitro* stability (see below). The Arg residue at position H66 (numbering according to Kabat *et al.* (26)) is far away from the antigen binding pocket and usually forms a double hydrogen bond to Asp(H86). Arg at position H66 was shown previously to result in higher protein stability than a Lys in the levan binding A48 scFv fragment (27, 28). Moreover, a Val-Ala variant of the anti-GCN4 scFv fragment (termed anti-GCN4(SS[--], with the subscripts indicating the absence of both disulfides)] was tested, where both intradomain disulfides were replaced by Val-Ala pairs (L-C23V, L-C88A, H-C22V, H-C92A). These mutations had been previously shown to act slightly stabilizing compared with the reduced dithiol form of the p185HER2-binding 4D5 scFv fragment, and it had been speculated that they might improve the performance of intrabodies (29).

Two additional variants were engineered by grafting (30) the anti-GCN4 wild-type CDR (complementary determining region) loops to another framework. As the acceptor framework we chose the so-called "hybrid" scFv (31). This acceptor framework is composed of the V_L domain of the 4D5 scFv fragment and the V_H domain of the A48[++](H2) scFv fragment, with the superscript indicating the presence of both disulfide bonds. It had been rationally designed from a series of stabilized domains and stands out for its extraordinary stability, as demonstrated by denaturant induced equilibrium unfolding, and a high expression yield (31). Two CDR-grafted variants with the anti-GCN4 scFv CDRs and the hybrid scFv framework were prepared by total gene synthesis. As the anti-GCN4 wild-type loop donor carried a λ light chain, while the acceptor hybrid framework carried a κ light chain, the loop grafting was not straightforward. Therefore, two different variants were designed, one more "κ-like" (termed κ-graft), the other more "λ-like" (termed λ-graft) (see Fig. 1). These two variants differ only in seven residues in the V_H-V_L interface region (Fig. 1d), potentially in-

fluencing the orientation of the two domains to each other. The design of the two graft variants is described in more detail in the following section and discussed later. The ampicillin-binding scFv fragment AL5[2] served as a negative control for a scFv fragment not binding Gcn4p.

Design of CDR-grafted Anti-GCN4 scFv Fragments

The structures of the anti-GCN4 antibody and the 4D5-A48 hybrid scFv were predicted by homology modeling using the Homology, Biopolymer, and Discover modules of the program InsightII version 95 (Biosym/MSI, San Diego, CA). The anti-GCN4 V_L model was based on the structure of antibody B1–8 (PDB entry 1a6v, 1.8-Å resolution, 96% sequence identity, 98% similarity). The V_H domain was modeled after the structure of antibody nmc-4 (PDB entry 1oak, 2.2-Å resolution, 86% identity, 90% similarity). The hybrid V_L domain is almost identical to the 4D5 version 8, PDB entry 1fvc, 2.2-Å resolution, 98% identity, 99% similarity) and the hybrid V_H domain model was based on the structure of antibody J539 (PDB entry 2fbj, 1.95-Å resolution, 85% identity, 87% similarity). Additional templates were used to model the CDR3 loops of the heavy chains. The V_L and V_H domains of the loop donor anti-GCN4 were superimposed on the corresponding domains of the framework donor (the 4D5-A48 hybrid), using a least squares fit of the Cα-coordinates of residues L3–L7, L20–L24, L33–L39, L43–L49, L62–L66, L71–L75, L84–L90, and L97–L103 (V_L) and residues H3–H7, H20–H24, H35a–H40, H44–H50, H67–H71, H78–H82, H88–H94, and H102–H108 (V_H), which represent the structurally least variable positions of the Ig variable domains. The sequences of the loop donor and the framework donor are very dissimilar: 43% identity (49% similarity) in the case of the V_L (one a λ and the other a κ chain) and 47% identity (69% similarity) in the case of V_H. The sequence of the two grafts (Fig. 1d) was determined by detailed analysis of the potential structural effects of any residue substitution.

Cloning, Expression, and Purification of scFv Fragments

All scFv fragments were in a V_L-V_H orientation with a 20-mer linker (GGGGSGGGGSGGGGSSGGGS) and a C-terminal His$_5$-tag. The scFv fragments expressed in yeast were cloned into the pESBA-Act expression vector, which carries a 2μ origin with a *TRP1* selection marker and a constitutive actin-1 promoter[3] (detailed information available upon request). All scFv fragments were cloned via *Bsp120I* and *StuI* restriction sites and carried a C-terminal His$_5$-tag. Two amino acids (Gly-Pro) encoding the *Bsp*120I site had to be included at the N terminus, after the initiating Met residue.

In vitro stability measurements of the different scFv fragments were performed with purified protein, expressed in bacteria. The anti-GCN4 wild-type was cloned into the expression vector pAK400 (32) and periplasmically expressed in *E. coli* JM83 (λ^-, *ara*, Δ(*lac, proAB*), *rpsL*, *thi*, Φ80, *dlacZ*ΔM15) at 25 °C (33). The H-R66K mutant, the two different graft variants as well as the hybrid framework, which were also periplasmically expressed under the same conditions, were cloned into the expression vector pIG6 (34). The Val-Ala variant of anti-GCN4 was cloned into the expression vector pTFT74 (34, 35) and cytoplasmically expressed as insoluble inclusion body protein in *E. coli* BL21DE3 (F^-, *ompT*$^-$, $r_B^- m_B^-$ (λimm21, *lac*I, *lac*UV5, *T7 pol, int*)) (36).

Periplasmically expressed scFv fragments were purified by immobilized metal ion affinity chromatography (making use of the C-terminal His$_5$-tag) and further purified by affinity chromatography on GCN4–7P14P as described (23). Refolding of the cytoplasmically expressed anti-GCN4(SS[--]) was attempted at three different pH values (pH 7.0, 8.0, and 9.0) as described for the disulfide-free A48 variants (27) and the 2-fold diluted refolding mixture was directly purified by affinity chromatography. Buffer exchange for all purified proteins was performed via PD-10 gel filtration columns from Amersham Pharmacia Biotech after concentrating the peak fractions eluting from the affinity column in Centriprep concentrators from Millipore.

In Vitro Analysis of scFv Fragments Expressed in Escherichia coli

Guanidinium-induced Equilibrium Unfolding—GdnHCl-induced denaturation was followed by recording the intrinsic fluorescence emission spectra of the proteins. Excitation was at 280 nm. Measurements were performed and analyzed as described before (27). Protein concentrations were 5 μg/ml in all cases and all measurements were performed in 40 mM Tris-HCl (pH 8.0), 150 mM NaCl at 20 °C, using a Shimadzu RF-5000 spectrofluorimeter. Denaturation curves were normalized as described (31). In principle, an estimate of the free energy of folding can

---

FIG. 1. **Sequences and structural models of CDR grafted scFv variants.** *a,* superposition of models for anti-GCN4 (*black*, CDR donor) and hybrid (*white*, CDR acceptor and framework donor) V_L and V_H fragment. *OL* denotes the outer loop. *b,* superposition of anti-GCN4 (*black*) and hybrid Fv fragment (*white*). *c,* λ-graft: the *black trace* indicates CDR regions according to Kabat *et al.* (26), *black spheres* the positions which actually differ from the hybrid sequence in both grafts. The additional mutations of dimer interface residues introduced in the creation of the λ-graft are indicated by ball-and-stick side chains. The V_H framework is shown in *white*, the V_L framework in *gray*. *d,* sequence alignment of models to the modeling templates. Residues different in the template are denoted as *white letters* on *black background*. The two grafts are aligned to the CDR donor (anti-GCN4 wild-type) and the framework donor (hybrid) sequence. Positions identical in all four sequences are highlighted by a *gray* background, sequence positions identical to the CDR donor sequence by *white letters* on a *black background*. *Black asterisks* on *white background* indicate framework residues which have been taken from the CDR donor in one or both of the grafts. *White asterisk* on *black background* indicates a residue formally denoted CDR2 which has been taken from the hybrid framework.

be obtained from equilibrium denaturation curves (37). However, the free energy calculation was not performed for the proteins under investigation, as this calculation requires the proteins to follow a two-state transition or at least two clearly separable transitions, which was clearly not the case for all scFv fragments. In a series of multiple transitions the scFv loses its functionality with the first transition. Thus, the estimated onset of denaturation in the transition curves (arbitrary defined as the GdnHCl concentration, where the normalized emission maximum was 0.05, see Fig. 2) was used as a semiquantitative estimate of *in vitro* stability. This procedure clearly does not provide an exact quantitative estimate of thermodynamic stabilities, but it does allow a qualitative ranking of *in vitro* stabilities for all different scFv variants.

Affinity Measurements—Antigen binding affinities of anti-GCN4, anti-GCN4(H-R66K), and the λ variant of the graft were determined in solution by the inhibition BIAcore method as described previously (23), with K_D and the active scFv concentration as variables to be fitted. Measurements were performed in duplicate in HBST buffer at pH 7.2, and averaged values are given. Preliminary enzyme-linked immunosorbent assay (ELISA) measurements (data not shown) had indicated that the κ-graft variant was of much lower affinity than the other scFvs.

Therefore, the affinity determination by the inhibition BIAcore method would have required prohibitive amounts of sample. Instead, the affinity of this mutant was determined directly from kinetic analysis with scFv concentrations between 1 and 400 nM. Even though all scFvs were analyzed by SMART gel chromatography and found to be monomeric at 100 μg/ml (data not shown), the kinetic analysis of the κ-graft variant suggests scFv dimerization occurring for this variant on the immobilized antigen in the flow cell, using the same chip as for the inhibition BIAcore (23). The kinetics were evaluated with a dimerizing analyte model, in which both monomer and dimer are allowed to bind, using a global fit with the program CLAMP (38, 39). While the global fit demands the dissociation constant of the monomer to be in the low micromolar range (consistent with the ELISA data; data not shown), there is some uncertainty about the exact value due to the complexity of the kinetics.

Integration of a Reporter Gene into the Chromosome of S. cerevisiae

The integrating reporter plasmid pAB183 was derived from pJP161 (40) by cloning two Gcn4p-binding sites at position 150 upstream of the
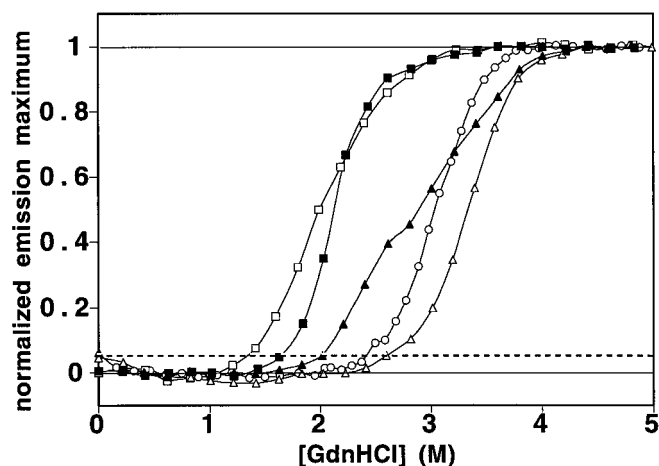
FIG. 2. **GdnHCl induced equilibrium unfolding transitions of different Gcn4p-binding scFv fragments.** Anti-GCN4 wild-type (■), destabilized point mutant anti-GCN4(H-R66K) (□), acceptor hybrid framework for CDR grafting (○), λ variant of graft (▲), κ variant of graft (▲). Unfolding was followed by the change in fluorescence emission maximum (excitation 280 nm). For better comparison, unfolding curves are normalized. The shift of the emission maximum is plotted from its initial baseline value (set to 0) to its final baseline value at high GdnHCl concentration (set to 1). The onset of denaturation (which was arbitrary defined as the GdnHCl concentration, where the normalized emission maximum is 0.05, as indicated by the *dotted line*) is shifted to higher denaturant concentrations, reflecting increased *in vitro* stability, in the order anti-GCN4(H-R66K), anti-GCN4 wild-type, λ-graft, acceptor framework, κ-graft. *Solid lines* indicate the normalized emission maximum of completely native and denatured protein, respectively.

TATA box of the GAL1 promoter. The Gcn4p-binding sites were generated by annealing two complementary oligonucleotides having a 5′ *Sph*I and 3′ *Sal*I compatible overhang sequence. The oligonucleotides are as follows: 5′-CCTATGACTCATCCAGTTATGACTCATCG-3′; 5′-TCGAC-GATGAGTCATAACTGGATGAGTCATAGGCATG-3′. This reporter plasmid was linearized at the *Apa*I site and integrated into the yeast genomic URA3 locus of strain JPY5 (40), resulting in YAdM2x*GCN4* −150. Four independent yeast transformants were tested in a functional assay, and all showed the same *GCN4*-dependent reporter gene activity. One of the clones (YAdM2x*GCN4* −150) was chosen for all subsequent experiments and is called yeast wild-type (to be distinguished from the *gcn4* knock-out strain).

Preparation of gcn4 Knock-out Strain

Disruption of the endogenous *GCN4* gene was performed by replacing the *GCN4* open reading frame with the kanMX4 module, according to the PCR-based gene deletion strategy described by Wach *et al.* (41). The kanMX4 module was amplified by PCR using primers homologous to either upstream sequences of the *GCN4* open reading frame (*GCN4* uptag primer: 5′-GTTTCGGCTCGCTGTCTTACCTTTTAAAATCTTCT-ACTTCTTGACCGTACGCTGCAGGTCGAC-3′) or downstream (*GCN4* downtag primer: 5′-CAGAACATACGGCAGATTATAAATGCGTGGTG-TAAAATTCTACTTATCGATGAATTCGAGCTCG-3′). YAdM2x*GCN4* −150 was transformed with the PCR product using the lithium acetate method, following standard protocols, to generate YAdM2x*GCN4* −150, *gcn4*::KAN. Transformants were grown on YPD plates for 24 h and subsequently replica plated on YPD plates containing 200 μg/ml geneticin (G418). Deletion of the *GCN4* open reading frame was confirmed for eight G418-resistant clones by analytical PCR of genomic DNA with primers annealing in the kanMX4 cassette and the flanking genomic regions on both sides of the integration site.

Cloning of GCN4 and 7P14P Leucine Zipper Mutant

The open reading frame of *GCN4* flanked by 1.25-kilobase upstream regulatory and 300-base pair downstream sequences was initially amplified by PCR using Pfu Polymerase (Stratagene) and yeast genomic DNA as template. The primers contain a *Sph*I site convenient for cloning into YEplac 181 (42), resulting in pAdM012*gcn4-2μ*.

The complete *GCN4* protein coding sequence was then amplified by PCR (Pfu Polymerase, Stratagene) from yeast genomic DNA with primers containing a *Hin*dIII site and cloned into pGAD424 (CLONTECH),

resulting in pAdM008. Substitution of Asp-255 and Ser-262 into prolines (corresponding to positions 7 and 14 of the leucine zipper domain, named 7P14P (24)) was performed by site-directed mutagenesis using pAdM008 as template for the PCR reaction. This mutant *GCN4* was subsequently cloned into pGAD424 (CLONTECH) resulting in pAdM010. In order to express the *GCN4* mutant under its own promoter, pAdM012*gcn4-2μ* and pAdM010 were digested with *Bam*HI-*Sph*I, and the appropriate *Sph*I-*Bam*HI DNA fragments of about 1.4 kilobases from pAdM010 and 1.3 kilobases from pAdM012*GCN4-2μ* were subcloned into Yeplac181 (42) linearized with *Sph*I.

In Vivo Analysis of scFv Fragments: Expression of scFv Fragments in Yeast and the β-Galactosidase Reporter Assay

The β-galactosidase assay in solution was performed using permeabilized cells as described (43). Activity was normalized to the number of cells assayed. All measurements were performed in triplicate, and averaged values are given.

The β-galactosidase reporter assay was performed with the different scFv fragments expressed in the wild-type yeast strain as well as in a *gcn4* deletion strain. Experiments in the knock-out strain were done in the absence of any *GCN4*, in the presence of *GCN4* episomally expressed on the pAsM012*GCN4* −2μ plasmid, or in the presence of the mutant form 7P14P of *GCN4* (24), unable to dimerize, expressed in the same vector. The reporter activity in the absence of any scFv was about 2-fold higher in the wild-type strain than in the knock-out strain harboring pAdM012*GCN4-2μ* plasmid and expressing *GCN4* in-trans (data not shown). Thus, normalized β-galactosidase activity driven by either endogenous *GCN4* or episomal *GCN4* expressed from pAdM012*GCN4* −2μ was arbitrarily set to 100% to compare the relative effects of coexpressed scFv variants in the wild-type and *gcn4* knock-out yeast strain.

Western Blot Analysis of Anti-GCN4 scFv Fragments

The solubility of the different anti-GCN4 scFv fragments was analyzed by Western blot. Five-ml cultures were grown at 30 °C to an optical density of about 2–3. Cells were normalized to the same cell densities, pelleted, and whole cell protein was extracted with Y-PER™ Yeast Protein Extraction Reagent form Pierce, which is a mild detergent formulation facilitating gentle isolation of soluble proteins. Soluble and insoluble fractions were separated by centrifugation (13,000 × g, 10 min, 4 °C). Samples of soluble and insoluble crude extract were subjected to SDS-polyacrylamide gel electrophoresis and blotted on polyvinylidene fluoride membranes, following standard protocols. His$_5$-tagged scFv fragments were detected with anti-His$_5$ scFv-AP fusion as described (44), with the chemiluminescent phosphatase substrate CSPD from Roche Molecular Biochemicals. To obtain reasonable intensities on the Western blots, about 5 times higher protein concentrations had to be used in the soluble fractions, compared with the insoluble fractions and the blots were exposed for different time spans. Thus, a direct comparison is only meaningful between all soluble or all insoluble samples, respectively.

Surface Plasmon Resonance Analysis of Soluble Fractions from Yeast Lysates

The soluble fractions of yeast lysates expressing the λ-graft, anti-GCN4 wild-type, anti-GCN4(SS^{--}), anti-GCN4(H-R66K), and no scFv ("empty vector") were, in addition to the Western blot analysis, applied to the same BSA leucine zipper-coated BIAcore chip used for the affinity measurements (see above). Because of its low affinity, the κ-graft was not tested in this experimental setup.

Soluble fractions of crude yeast lysates, normalized to same cell densities, were prepared as described in the previous section and diluted 1:250 into HBST buffer in the presence or absence of 10^{-7} M soluble antigenic peptide. Samples were preincubated for 1 h on ice and injected for 600 s over BSA leucine zipper-coated chips as described previously (23). For each protein, the curve in the presence of antigenic peptide was subtracted from the corresponding curve in the absence of antigenic peptide. The corrected curves were set to zero at the time point of injection and plotted against the time after injection.

RESULTS

Bacterial Expression and Purification of scFv Fragments—The expression yields of the periplasmically expressed Gcn4p-binding scFv fragments were in the range of 0.5–3 mg of purified protein per liter of *E. coli* JM83. In the case of the κ-graft, significantly more scFv protein was expressed and eluted after

the initial immobilized metal ion affinity chromatography column (see "Experimental Procedures") than in the case of all other Gcn4p-binding scFv fragments, similar as for the very well expressing hybrid scFv framework donor (31). However, in the subsequent antigen-affinity purification step, very little κ-graft bound to the column, probably due to the low affinity of this variant (see below). When reloading the flow-through from the affinity column, again a similar small amount of the κ-graft bound to the column, indicating that binding was affinity-limited. In contrast, the λ-graft bound to the column normally, consistent with its high affinity (see below). The cysteine-free anti-GCN4(SS⁻⁻) scFv, which was refolded from inclusion bodies, could not be analyzed *in vitro*, as it was extremely aggregation prone, impeding the concentration steps and buffer change necessary for further experiments.

The in Vitro Stabilities of the Analyzed scFv Fragments Differ Significantly—The *in vitro* stabilities were tested by measuring GdnHCl-induced equilibrium unfolding. The equilibrium unfolding transitions of the analyzed scFv fragments are superimposed in Fig. 2. Since several of the fragments clearly do not follow two-state transitions, the calculation of free energies is not possible for all of them. To be able to compare all of them semiquantitatively, their onset of denaturation was measured. The anti-GCN4 wild-type scFv fragment started denaturing at about 1.7 M GdnHCl (*filled squares*). The destabilized point mutant with the H-R66K mutation had its onset of denaturation shifted to about 1.4 M GdnHCl, and the transition curve was flattened (*open squares*). The λ-graft was found to be more stable than the anti-GCN4 wild-type and had its denaturation onset shifted to about 2.0 M GdnHCl (*filled triangles*). This graft variant appeared to form an equilibrium intermediate, resulting in a step in the transition curve at about 2.75 M GdnHCl, with V_L denaturation preceding V_H denaturation (31). This interpretation could be further strengthened by destabilizing the V_L domain in the λ-graft (by using a variant in which the outer loop, *i.e.* residues L66 to L71, have been taken from the framework donor hybrid scFv and in which the additional mutation Val(L36) to Tyr is introduced), which shifted the lower curve part to lower denaturant concentrations, resulting in a distinct plateau region in the transition curve (data not shown). The λ-graft variant was thus less stable than the acceptor hybrid framework (*open circles*), but its first transition started clearly at higher denaturant concentrations than in anti-GCN4 wild-type protein. The κ-graft appeared to be even more stable than the hybrid framework with an onset of denaturation around 2.6 M (*open triangles*). Fluorescence emission maxima of native proteins were between 339 and 340 nm, while all denatured proteins showed an emission maximum of about 350 nm. The semiquantitative stability comparisons have been performed with the different scFv fragments in the presence of their disulfide bonds. However, most likely all scFv fragments will be destabilized by about the same amount if the disulfide bonds do not form, since the core structure of antibody variable domains is highly conserved, such that the proposed stability ranking of the different mutants should not change.

The Two Graft Variants Show Remarkable Differences in Antigen Binding Affinity—The affinities of the anti-GCN4 wild-type scFv, the destabilized point mutant, and the two framework-engineered graft variants to the 7P14P leucine zipper peptide were measured in solution by inhibition BIAcore (23) or by binding kinetics. The K_D of the anti-GCN4 wild-type was determined to be $(4.4 \pm 0.1) \times 10^{-11}$ M, in good agreement with values determined before (23). The destabilized point mutant H-R66K had an essentially identical affinity, as expected from the position of this mutation in the model structure, which is distant from the binding pocket (27), and the K_D was deter-
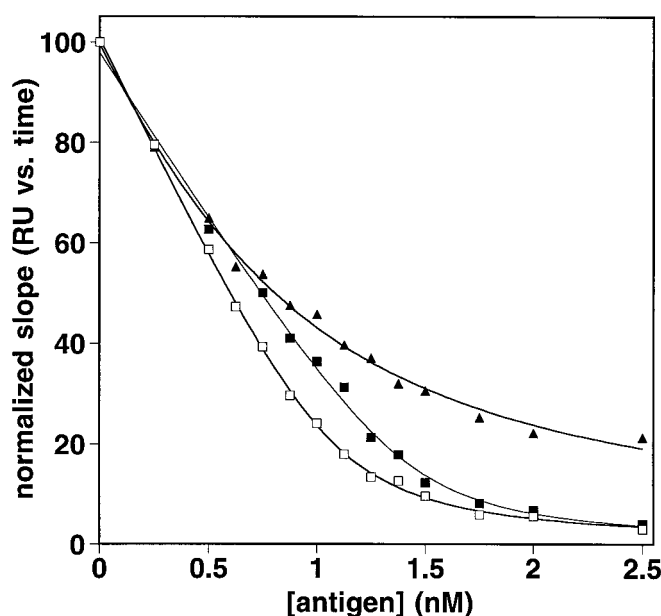

FIG. 3. **Determination of antigen dissociation constants (K_D) in solution of anti-GCN4 wild-type (■), anti-GCN4(H-R66K) (□), and λ-graft (▲) scFv fragments by inhibition BIAcore.** Purified proteins at 1 nM concentration were mixed with different concentrations of GCN4(7P14P) peptide and injected over a BSA-GCN4(7P14P)-coated chip. From the linear sensograms, the slopes (resonance units (*RU*) *versus* time) were plotted against the corresponding total soluble antigen concentration. The slopes are normalized to 100%, representing the corresponding slopes in the absence of any antigen. K_D values were fitted as described in the text. Even though the curves for the wild-type (■) and the H-R66K mutant (□) look slightly different, they fit to essentially the same K_D (Table I) as the concentration of active scFv was slightly different. The curves represent the results from single measurements out of duplicate repeats of the whole experiment. The errors for duplicate measurements and the numerical K_D values are given in Table I.

mined to be $(4.2 \pm 2.7) \times 10^{-11}$ M. The λ-graft had a K_D of $(3.8 \pm 0.8) \times 10^{-10}$ M, about 1 order of magnitude weaker than the anti-GCN4 wild-type. The titration curves are overlaid in Fig. 3, where the slopes are plotted against the corresponding total antigen concentration for these three variants (anti-GCN4 wild-type, anti-GCN4(H-R66K) and λ-graft).

A significantly weaker affinity was determined for the κ-graft variant ($K_D \sim 2 \times 10^{-6}$ M). As the inhibition BIAcore method would have required large amounts of antigenic peptide in this case, the affinity of the κ-graft was determined by direct fitting from the on- and off-rates, as described under "Experimental Procedures." This weak affinity indicates that the maintained κ framework residues (Fig. 1) do perturb the conformation of the λ-CDRs or change the relative domain orientation, necessary for an optimal orientation of the V_H and V_L CDR loops to each other. The low affinity of the κ-variant in the micromolar range is consistent with its very weak signal in anti-His₅ tag inhibition ELISA (data not shown) and the poor binding of this variant to the affinity column (see above).

Anti-GCN4 scFv Intrabodies Inhibit the Transactivation Potential of Gcn4p—The anti-GCN4 scFv was initially tested for its biological activity expressed from several yeast vectors including *GAL1* and *ADH*-driven promoters. In addition, the nuclear localization signal from SV40 large T-antigen was fused N-terminal to the anti-GCN4 scFv. Of the combinations tested, the anti-GCN4 scFv showed the strongest biological effect when expressed from the actin-1 promoter without any nuclear localization signal using the pESBA-Act expression vector (see "Experimental Procedures") with *TRP1* selection marker and 2μ origin (data not shown). This vector was sub-
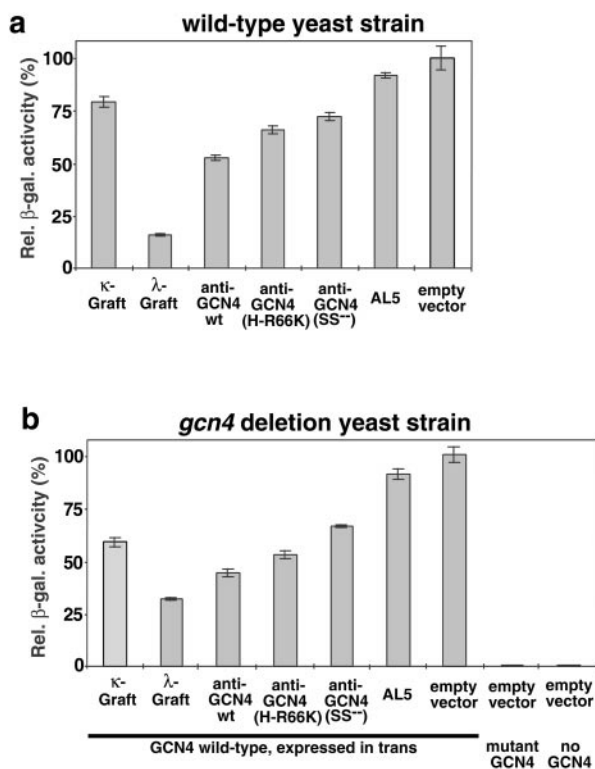
FIG. 4. *In vivo* **performance of different scFv fragments expressed in yeast.** The influence of different scFv variants on gene expression of a Gcn4p-dependent LacZ reporter gene was investigated in wild-type strain (*a*) and *gcn4* knock-out strain (*b*), in which Gcn4p was expressed in *trans*. The reporter construct contained two Gcn4p-binding sites at position −150 relative to the TATA box and was integrated into the yeast genome. Relative β-galactosidase activity (*rel. β-gal. activity*) driven by endogenous Gcn4p or episomally expressed Gcn4 was arbitrarily set to 100%. AL5 is an ampicillin-binding scFv fragment and serves as negative control. Besides the anti-GCN4 wild-type, a destabilized point mutant (anti-GCN4(H-R66K)), a cysteine-free variant of the anti-GCN4 wild-type (anti-GCN4(SS⁻⁻)), and two framework stabilized variants of anti-GCN4 (κ-graft and λ-graft) were tested in wild-type and *gcn4* knock-out strains. *a,* the stabilized λ-graft was the most active intrabody, while the destabilized H-R66K point mutant and the cysteine-free variant of anti-GCN4 showed decreased activity, compared with the anti-GCN4 wild-type. The decreased activity of the κ-graft is believed to be due to its low binding affinity (see Table I). *b,* same experiments as in *a,* however, in a *gcn4* knock-out strain with *GCN4* expressed in *trans* on a 2μ plasmid. Similar inhibition patterns were obtained. The background caused by monomeric *GCN4* binding to its binding sequence can be estimated from the mutant *GCN4* expressed in *trans*; Gcn4p independent reporter activity can be estimated from the reporter activity in the absence of coexpressed *GCN4*. Both backgrounds are negligible.

sequently used for all further experiments.

The *in vivo* effect of expressing the different scFv fragments on *GCN4*-dependent *lacZ* expression is depicted in Fig. 4. In the wild-type yeast strain (YAdM2x*GCN4* −150) (Fig. 4*a*), the unspecific AL5 control scFv caused no significant decrease in reporter gene activity. The framework stabilized λ-graft showed the strongest effect as intrabody, followed by the anti-GCN4 wild-type, resulting in a decrease of β-galactosidase activity to 16 and 52%, respectively. The highly stable but weakly binding κ-graft and the cysteine-free anti-GCN4(SS⁻⁻) caused only moderate decrease in reporter gene activity. This low activity of the κ-graft is most likely due to its low binding affinity (see Table I). The destabilized point mutant anti-GCN4 (H-R66K) was less efficient in inhibition of *GCN4*-dependent reporter gene activity, compared with the wild-type scFv. The pattern of Gcn4p transactivation inhibition was highly reproducible and was also confirmed when using a different assay

method, where β-galactosidase reporter activity was measured after disrupting the cells by glass beads or freeze-thaw cycles for lysis and normalizing the β-galactosidase activity to protein concentration (45) (data not shown). A similar inhibition pattern with an almost identical ranking of the different scFv mutants was also obtained in the *gcn4* deletion strain (YAdM2x*GCN4* −150, *gcn4*::KAN) with episomally expressed *GCN4* (Fig. 4*b*).

As controls, we also expressed the mutant 7P14P Gcn4p (see "Experimental Procedures"), unable to form functional homodimers, in the *gcn4* knock-out strain and as expected, no detectable reporter gene activity was observed ("empty vector, mutant GCN4" in Fig. 4*b*). Furthermore, no β-galactosidase activity was observed in the *gcn4* deletion strain in the absence of any Gcn4p, showing that the *lacZ* reporter was completely under the control of Gcn4p ("empty vector, no GCN4" in Fig. 4*b*). The onset of denaturation, binding affinity, and the effect on reporter gene activity in the wild-type yeast strain and *gcn4* knock-out strain with episomally expressed *GCN4* are summarized in Table I for scFv fragments anti-GCN4, anti-GCN4(H-R66K), λ-graft, and κ-graft.

Both Graft Variants Are Soluble in Yeast Cytoplasm—The solubility of the different Gcn4p-binding scFv fragments in yeast was tested by Western blot analysis. Only in case of the λ- and κ-graft variants significant amounts of soluble protein could be detected in crude cell extracts (Fig. 5). All other anti-GCN4 scFv fragments appeared to be essentially completely insoluble, with the amount of insoluble scFv slightly increasing with decreasing *in vitro* stability. The detection of soluble scFv protein, which was apparently present only in very low concentrations in most of the crude extracts, was hampered by some background binding obtained with the anti-His₅ scFv fragment, which binds to some yeast proteins present in the crude extract, when they are loaded at high concentration. Nevertheless, the observed dramatic difference in solubility between the graft variants and the remaining anti-GCN4 scFv fragments was highly reproducible.

Moreover, the difference between the λ-graft and the non-grafted anti-GCN4 variants in the amount of protein present in the soluble fraction of crude yeast cell extracts was also confirmed by SPR. In this experiment, soluble crude yeast lysate from cells expressing the respective scFv fragment was passed over the BIAcore chip coated at high density, such that a mass-transport limited rate is observed. To determine specific binding, the same experiment was carried out in the presence of inhibiting concentrations of antigenic peptide, and this curve is subtracted from the first. Only the curve of the λ-graft, injected over BSA leucine zipper-coated chip, had a significant slope after the background subtraction, indicating the presence of functional protein in the crude soluble fraction (Fig. 6). The slopes of anti-GCN4 wild-type, anti-GCN4(SS⁻⁻), and anti-GCN4(H-R66K) were not convincingly different from the empty vector control (Fig. 6). This control experiment rules out the possibility that a meaningful amount of functional protein might have been present in the soluble crude fractions of anti-GCN4 wild-type, anti-GCN4(SS⁻⁻), and anti-GCN4(H-R66K), which would not have been detected by Western blot analysis, because of a potential proteolytical removal of the His₅-tag in the crude fractions. Instead, we found similar results from the Western blot (Fig. 5) and the SPR analysis (Fig. 6).

One has to caution, however, that the exact ratio of soluble to insoluble protein for the different scFv variants may not necessarily reflect the ratio present *in vivo*. It cannot be excluded that part of the different anti-GCN4 variants might have precipitated during sample preparation, even though we used a gentle cell disruption method, by using the Y-PER™ Yeast

The *in vivo* performance correlated with the *in vitro* stability, as long as a certain minimum affinity was surpassed. Errors represent mean ± S.D. ($n = 3$ in β-galactosidase assays; $n = 2$ in K_D determinations). Dissociation constants (K_D) were determined by BIAcore. *In vivo* activities were determined by measuring β-galactosidase activities in permeabilized yeast cell cultures, either in the wild-type or in the *gcn4* knock-out yeast strain. Activities are normalized to reporter gene activity in the absence of coexpressed scFv fragment, which was set to 100%. Thermodynamic stabilities were determined semiquantitatively by giving the approximate onset of denaturation, estimated from GdnHCl denaturation curves, as not all fragments followed two-state transitions.

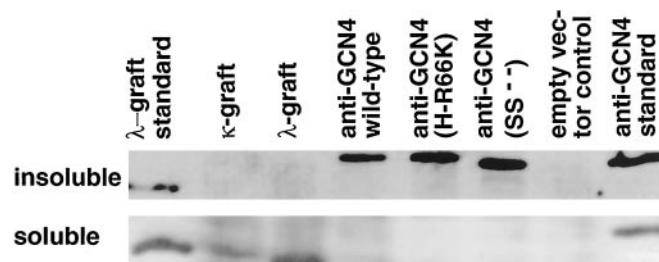| Protein	K_D	Measured β-galactosidase activity (wild-type yeast)	Measured β-galactosidase activity (*gcn4* knock-out yeast)	Approximate onset of denaturation
	M	*%*	*%*	*GdnHCl, M*
Anti-GCN4 wt	$(4.4 \pm 0.1) \times 10^{-11}$	52 ± 1.4	44 ± 1.9	1.7
Anti-GCN4(H-R66K)	$(4.2 \pm 2.7) \times 10^{-11}$	66 ± 2.0	53 ± 1.8	1.4
λ-Graft	$(3.8 \pm 0.8) \times 10^{-10}$	16 ± 0.5	32 ± 0.6	2.0
κ-Graft	$\sim 2 \times 10^{-6}$	79 ± 2.4	59 ± 2.1	2.6

FIG. 5. **Western blot analysis of solubility of different Gcn4p-binding scFv fragments expressed in yeast.** scFv fragments were detected by anti-His$_5$-tag AP fusion. The κ- and λ-graft variant run at about identical positions, as do the anti-GCN4 wild-type, (H-R66K) mutant, and anti-GCN4(SS^{--}). Purified protein recombinantly expressed in *E. coli* was used for the respective controls in the lanes labeled "λ-graft standard," respectively, "anti-GCN4 standard." The empty vector control was prepared from yeast extract without expressed scFv fragment. While the graft variants were only detectable in the soluble fraction of crude extract, anti-GCN4 wild-type, anti-GCN4(H-R66K), and anti-GCN4(SS^{--}) were detectable only in the insoluble fraction. Note that a direct quantitative comparison between insoluble and soluble fractions is not appropriate, since the soluble fractions were prepared from about 5 times higher concentrated cell extract and the "soluble" and "insoluble" blots have been exposed for different time spans.
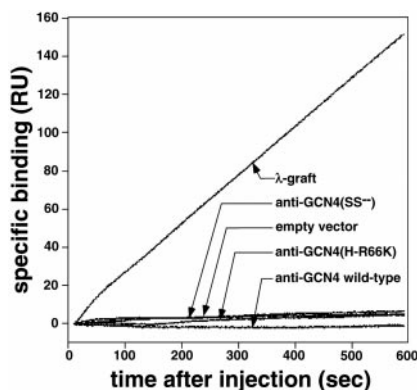

FIG. 6. **SPR analysis of soluble crude yeast extracts expressing λ-graft, anti-GCN4 wild-type, anti-GCN4(SS^{--}), anti-GCN4 (H-R66K), and no scFv (empty vector).** Soluble fractions were prepared as described in the text, diluted 1:250 into HBST buffer, and injected for 600 s over BSA leucine zipper-coated chip in the presence or absence of 10^{-7} M soluble antigenic peptide. The amount of functional scFv fragment (specific binding in resonance units, *RU*) is indicated by having subtracted the curve in the presence of antigenic peptide from the corresponding curve in the absence of antigenic peptide for each protein. These difference curves are shown and have been normalized to zero RU at the time point of injection.

Protein Extraction Reagent form Pierce. Furthermore, the soluble protein may be short lived, either through precipitation or proteolysis. Thus, it would be no more detectable in the crude lysate, but can still have a modest inhibitory effect on GCN4 under conditions of continuous synthesis in the growing cell.

DISCUSSION

In the present study we have investigated the interplay between *in vitro* stability, affinity, and the performance of cytoplasmically expressed scFv intrabodies. Fragments with essentially identical affinities but slight differences regarding *in vitro* stability, such as the anti-GCN4 wild-type and its destabilized H-R66K point mutant, performed *in vivo* corresponding to their *in vitro* stability (Fig. 4a). The variant with highest activity *in vivo* was the λ-graft. The increased activity of this fragment was not due to improved affinity, compared with the anti-GCN4 wild-type molecule, since the λ-graft had an affinity which was even weaker by about 1 order of magnitude (Table I, Fig. 3). Thus, increased *in vitro* stability appeared to be responsible for the improved effect. A higher fraction of scFv fragment with increased *in vitro* stability can fold correctly, even in the absence of the stabilizing intradomain disulfides, which do not form in the cytoplasm. In case of the λ-graft, the improved folding was also reflected in a larger amount of soluble scFv, detectable by Western blotting (Fig. 5) and SPR (Fig. 6).

The κ-graft performed significantly worse *in vivo* than the anti-GCN4 wild-type molecule (Fig. 4a). This graft variant, which differs in only 7 amino acid residues from the λ-graft (Fig. 1d), had an extraordinary high *in vitro* stability (Fig. 2), but only a rather low binding affinity, with a K_D in the micromolar range (Table I). Taken together, a high affinity is clearly required for the Gcn4p-binding intrabodies to be active *in vivo*. As soon as this threshold affinity was reached, further improvements of intrabody activity could predominantly be achieved by increasing the stability, and a correlation between *in vitro* stability and *in vivo* performance of fragments with similar affinities was observed.

Stabilization of scFv fragments for intracellular applications can either be achieved by introducing stabilizing point mutations (as, for example, Arg at position H66) or by CDR grafting onto a superior scFv framework, as performed for the framework-engineered λ-graft. The latter strategy has also been successfully employed for stabilizing a fluorescein-binding scFv fragment (46). Additionally, attaching a constant domain to the scFv fragments may also improve scFv stability, because constant domains may possibly provide additional extrinsic domain stabilization to the scFv. Although not tested by quantitative *in vitro* stability measurements yet, it is possible that it was this increased stability, which caused improved effects of cytoplasmically expressed intrabodies in some cases, where scFv constant domain fusions were expressed, and improved performance as cytoplasmic intrabodies was noticed (18, 47). However, it is also possible that increased folding yield is responsible for the improved effect of constant domain fusions,

Stability of Intrabodies

since the presence of the constant domain covers the hydrophobic V-C interface of the variable domain, which is solvent exposed in the scFv fragment and can contribute to aggregation (48).

The cysteine-free anti-GCN4(SS^{--}) scFv fragment caused a smaller decrease in reporter gene activity than the anti-GCN4 wild-type (Fig. 4a). Thus, the reduced dithiol form of the wild-type scFv intrabody, as present in the reducing environment of the cytoplasm, performed better *in vivo* than the anti-GCN4(SS^{--}). Replacing the disulfides in scFv fragments with Val-Ala pairs therefore does not necessarily cause an improved effect of cytoplasmically expressed intrabodies, even though Val-Ala pairs had been found to be slightly more stable compared with the reduced dithiol form of the 4D5 scFv fragment (29). However, apparently this effect is antibody-specific or overcompensated by the aggregation tendency of the cysteine-free variant, and these differences require a more detailed investigation.

The exact mode of action of the cytoplasmically expressed anti-GCN4 intrabodies is at present unknown. The target protein Gcn4p is synthesized in the cytoplasm, but acts in the nucleus by binding to its target sequence. In the normal yeast cell Gcn4p homodimerizes via its leucine zipper domain and is active as a dimer (20). The anti-GCN4 intrabody, directed against the monomeric random-coil form of the Gcn4p leucine zipper (24), should compete with Gcn4p homodimerization. Once bound, the intrabody may either impede transport of the complex into the nucleus, a mechanism of action previously suggested for other cytoplasmically expressed intrabodies (14). Alternatively, the complex may enter the nucleus and prevent dimerization and subsequent binding of Gcn4p to its target sequence there. Low affinity binders such as the κ-graft will only form marginally stable complexes with Gcn4p. Under equilibrium conditions, a higher fraction of Gcn4p molecules is likely to homodimerize, since the affinity of Gcn4p leucine zipper homodimerization is submicromolar (49, 50) and thus higher than the affinity of the κ-graft scFv fragment to the Gcn4p leucine zipper. This explains the weaker effect of the low affinity intrabody. Extremely high affinity scFv intrabodies, on the other hand, will "capture" Gcn4p almost irreversibly and prevent its homodimerization more efficiently, unless the antibody denatures or too little of the antibody is native in the first place. The increased activity of an intrabody with improved affinity has been reported before (51).

The design of the graft variants deserves some further discussion, since this is, to our knowledge, the first reported grafting from a λ CDR-loop donor to a κ acceptor framework. When performing a loop graft with the aim of humanizing an antibody and/or achieving improved stability and folding yields, one usually chooses a framework sequence which is reasonably similar to that of the loop donor. This strategy minimizes the effects that the differences in core packing and framework conformation could have on CDR conformation and thus on antigen binding affinity and selectivity. In grafting the Gcn4p-binding loops onto the extremely stable hybrid framework we did not have the option to heed this consideration: we had to graft between domains at opposite ends of the conformational range for immunoglobulin variable domains (Fig. 1a). In the case of V_L, the antigen binding characteristics had to be transferred from a λ-type V_L domain to a κ chain (43% sequence identity, 49% similarity). The V_H domains were rather dissimilar as well (47% identity, 69% similarity), the two domains belonging to two different structural subclasses. In addition, the relative orientation of the two domains in Fv fragments containing λ light chains is generally more variable than in those containing κ light chains. This is demonstrated in a superposition of the two models, one retaining the relative domain orientation of the λ modeling template used to model the anti-GCN4 V_L, the other with the domain orientation of the 4D5 structure used to model the hybrid κ V_L domain (Fig. 1b).

An analysis of the types of sequence changes which would be needed to retain the antigen binding characteristics revealed that, in addition to a classical graft of the CDR loops, at least the buried residues of the fourth, outer loop (residues L66 to L71, Fig. 1) would need to be retained from the anti-GCN4 sequence, since these residues interact with CDR1. In addition, it seemed very likely that it would be necessary to retain a λ-like dimer interface, since a change in domain orientation would very likely interfere with binding. However, particularly the replacement of Gln(L38) (which is highly conserved in κ V_L sequences and whose side chain forms a double hydrogen bond across the dimer interface to the side chain of Gln(H39)) by Glu (which is encoded in the mouse $\lambda1$ germline gene) was very likely to destabilize the dimer interface. To test whether this was indeed the case, we designed two grafts, one retaining the loop donor's λ dimer interface (λ-graft), the other the framework donor's κ dimer interface (κ-graft). The core and particularly the N-terminal sequence with the one residue deletion at position L8, typical for λ chains, was in both cases changed to a κ-like structure (Fig. 1d). However, care had to be taken to prevent steric problems due to the different CDR1 conformation, which would have clashed with the outer loop, if this had not been changed to a λ-like sequence as well. The experimental results indicate that the λ-graft was finally the better solution, since it retained most of the binding affinity (Table I), although it was less stable than the κ-graft (Fig. 2).

The experiments in the *gcn4* deletion strain were performed to exclude that any background signal is caused by monomeric Gcn4p. Indeed, essentially no β-galactosidase activity was detectable with the Gcn4p mutant (Fig. 4b). The anti-GCN4 scFv fragments prevent dimerization of Gcn4p, but do not necessarily inhibit binding of a complex between monomeric Gcn4p and scFv fragment to the target sequence. Although it is known that Gcn4p acts as a dimer *in vivo* (20), monomeric Gcn4p was shown to be able to bind its specific DNA site *in vitro* with a diffusion limited on-rate (52). Therefore, the maximum decrease in reporter activity theoretically achievable should be the level caused by monomeric Gcn4p, which is in turn essentially undetectable. Since the binding sequence of monomeric Gcn4p is only 5 base pairs long and this repeat should statistically occur about 15,600 times in the yeast genome, evolution should have favored monomeric binding to be of low affinity, and thus this absence of any background binding by monomers is not surprising.

Coexpression of the λ-graft, the best performing intrabody, resulted in reporter activity still significantly higher than when monomeric 7P14P mutant Gcn4p was expressed, *i.e.* the theoretical optimum (see above). Thus, although a remarkable improvement compared with the anti-GCN4 wild-type could be achieved, there still appears to be room for further optimization. Possibly, further protein engineering for stability and affinity might cause additional improvement, particularly by increasing the expression yield of functional protein. Higher expression levels of cytoplasmic scFv fragments do, however, often result in increased aggregation, rather than an increased amount of functional protein (13). Moreover, it is likely that a complete functional knock-out will never be achievable in such a system, because the intrabody can probably not completely abolish Gcn4p homodimerization which may be too fast to be completely inhibitable, and the Gcn4p leucine-zipper dimer, once formed, is rather stable (49, 53) and may activate transcription before equilibrium binding to the antibody is reached.

No soluble protein could be detected in Western blot (Fig. 5) and SPR analysis (Fig. 6) of anti-GCN4 wild-type, its destabilized point mutant H-R66K and the cysteine-free anti-GCN4 variant. Nevertheless, these fragments produced a specific biological response, causing a decrease in reporter gene activity (Fig. 4). A similar situation with a seemingly completely insoluble cytoplasmically expressed intrabody, which was nevertheless active, has been reported before in the case of the p21^{ras} binding Y13–259 scFv fragment (54). It had been speculated that a partially folded form of the molecule might interact with the target antigen before precipitating. Alternatively, it is possible that only a very small fraction of these seemingly completely insoluble intrabodies, which is difficult to detect *in vitro*, is correctly folded and responsible for the measured biological effects or that the *in vitro* solubilities do not properly reflect the solubilities *in vivo*. For example, it is possible that in the growing yeast cell a higher steady state level of soluble scFv fragment can be reached than detectable in the soluble crude lysates, if the protein is proteolytically labile or slowly precipitating. This point will require further investigations.

Although it has been reported that the disulfide bridges do not form in the cytoplasm (10), our experiments do not allow to exclude the possibility that a trace of the scFv proteins escapes the cellular reduction machinery, becomes oxidized due to some oxygen diffusing into the cell, and is responsible for most of the observed inhibitory effects. Such a scenario could potentially explain the surprising effect that the λ-graft and the wild-type do differ less dramatically in their inhibitory effect on reporter gene activity (Fig. 4a) than one might have expected based on the significant differences in solubility (Fig. 5). This might also explain the poor performance of the cysteine-free variant.

The apparent all or nothing effect in intrabody solubility (Fig. 5) suggests that the graft variants may have an intrinsically higher solubility, compared with the three other anti-GCN4 variants. Protein aggregation is believed to start mainly from folding intermediates, rather than from the native structure (55). The formation of these intermediates, starting from correctly folded protein, is often closely related to the thermodynamic stability of the native state (31, 56). However, differences in the solubility of the native state or the intermediates themselves may also play a role. The difference in activity between the anti-GCN4 wild-type and the destabilized point mutant H-R66K, which both appeared to be completely insoluble (Fig. 5) and have about identical affinities (Table I, Fig. 3) provides additional evidence for the proposed direct linkage between the *in vitro* thermodynamic stability and the *in vivo* performance of cytoplasmic intrabodies.

In summary, increasing the stability of cytoplasmically expressed scFv intrabodies was shown to result in fragments with significantly improved *in vivo* performance. Thus, stability engineering appears to be a challenge of high priority to further improve the promising effects of many cytoplasmically expressed scFv fragments for potential future biochemical and therapeutic applications.

REFERENCES

1. Bird, R. E., Hardman, K. D., Jacobson, J. W., Johnson, S., Kaufman, B. M., Lee, S., Lee, T., Pope, S. H., Riordan, G. S., and Whitlow, M. (1988) *Science* **242,** 423–426
2. Huston, J. S., Levinson, D., Mudgett-Hunter, M., Tai, M., Novotny, J., Margolies, M. N., Ridge, R. J., Bruccoleri, R. E., Haber, E., Crea, R., and Oppermann, H. (1988) *Proc. Natl. Acad. Sci. U. S. A.* **85,** 5879–5883
3. Carlson, J. R. (1988) *Mol. Cell. Biol.* **8,** 2638–2640
4. Biocca, S., and Cattaneo, A. (1995) *Trends Cell Biol.* **5,** 248–252
5. Marasco, W. A. (1995) *Immunotechnol.* **1,** 1–19
6. Martineau, P., Jones, P., and Winter, G. (1998) *J. Mol. Biol.* **280,** 117–127
7. Gilbert, H. F. (1990) *Adv. Enzymol. Relat. Areas Mol. Biol.* **63,** 69–172
8. Williams, A. F., and Barclay, A. N. (1988) *Annu. Rev. Immunol.* **6,** 381–405
9. Proba, K., Honegger, A., and Plückthun, A. (1997) *J. Mol. Biol.* **265,** 161–172
10. Biocca, S., Ruberti, F., Tafani, M., Pierandrei-Amaldi, P., and Cattaneo, A. (1995) *Bio/Technology* **13,** 1110–1115
11. Goto, Y., and Hamaguchi, K. (1979) *J. Biochem.* (*Tokyo*) **86,** 1433–1441
12. Frisch, C., Kolmar, H., Schmidt, A., Kleemann, G., Reinhardt, A., Pohl, E., Usón, I., Schneider, T. R., and Fritz, H.-J. (1996) *Fold. Des.* **1,** 431–440
13. Cattaneo, A., and Biocca, S. (1999) *Trends Biotech.* **17,** 115–121
14. Duan, L., Bagasra, O., Laughlin, M. A., Oakes, J. W., and Pomerantz, R. J. (1994) *Proc. Natl. Acad. Sci. U. S. A.* **91,** 5075–5079
15. Mhashilkar, A. M., Bagley, J., Chen, S. Y., Szilvay, A. M., Helland, D. G., and Marasco, W. A. (1995) *EMBO J.* **14,** 1542–1551
16. Gargano, N., and Cattaneo, A. (1997) *J. Gen. Virol.* **78,** 2591–2599
17. Biocca, S., Pierandrei-Amaldi, P., Campioni, N., and Cattaneo, A. (1994) *Bio/Technology* **12,** 396–399
18. Cohen, P., Mani, J. C., and Lane, D. P. (1998) *Oncogene* **17,** 2445–2456
19. Landschulz, W. H., Johnson, P. F., and McKnight, S. L. (1988) *Science* **240,** 1759–1764
20. Hope, I. A., and Struhl, K. (1987) *EMBO J.* **6,** 2781–2784
21. Hinnebusch, A. G. (1997) *J. Biol. Chem.* **272,** 21661–21664
22. Albrecht, G., Mösch, H.-U., Hoffmann, B., Reusser, U., and Braus, G. H. (1998) *J. Biol. Chem.* **273,** 12696–12702
23. Hanes, J., Jermutus, L., Weber-Bornhauser, S., Bosshard, H. R., and Plückthun, A. (1998) *Proc. Natl. Acad. Sci. U. S. A.* **95,** 14130–14135
24. Leder, L., Berger, C., Bornhauser, S., Wendt, H., Ackermann, F., Jelesarov, I., and Bosshard, H. R. (1995) *Biochemistry* **34,** 16509–16518
25. Berger, C., Weber-Bornhauser, S., Eggenberger, J., Hanes, J., Plückthun, A., and Bosshard, H. R. (1999) *FEBS Lett.* **450,** 149–153
26. Kabat, E. A., Wu, T. T., Perry, H. M., Gottesman, K. S., and Foeller, C. (1991) *Sequences of Proteins of Immunological Interest,* NIH Publication 91-3242, National Technical Information Service, Springfield, VA
27. Proba, K., Wörn, A., Honegger, A., and Plückthun, A. (1998) *J. Mol. Biol.* **275,** 245–253
28. Wörn, A., and Plückthun, A. (1998) *Biochemistry* **37,** 13120–13127
29. Wörn, A., and Plückthun, A. (1998) *FEBS Lett.* **237,** 357–361
30. Jones, P. T., Dear, P. H., Foote, J., Neuberger, M. S., and Winter, G. (1986) *Nature* **321,** 522–525
31. Wörn, A., and Plückthun, A. (1999) *Biochemistry* **38,** 8739–8750
32. Krebber, A., Bornhauser, S., Burmester, J., Honegger, A., Willuda, J., Bosshard, H. R., and Plückthun, A. (1997) *J. Immunol. Methods* **201,** 35–55
33. Knappik, A., Krebber, C., and Plückthun, A. (1993) *Bio/Technology* **11,** 77–83
34. Ge, L., Knappik, A., Pack, P., Freund, C., and Plückthun, A. (1995) in *Antibody Engineering* (Borrebaeck, C. A. K., ed) 2nd Ed., pp. 229–266, Oxford University Press, Oxford
35. Freund, C., Ross, A., Guth, B., Plückthun, A., and Holak, T. A. (1993) *FEBS Lett.* **320,** 97–100
36. Studier, F. W., and Moffatt, B. A. (1986) *J. Mol. Biol.* **189,** 113–130
37. Pace, C. N. (1990) *Trends Biotechnol.* **8,** 93–98
38. Morton, T. A., and Myszka, D. G. (1998) *Methods Enzymol.* **295,** 268–294
39. Myszka, D. G., and Morton, T. A. (1998) *Trends Biochem. Sci.* **23,** 149–150
40. Barberis, A., Pearlberg, J., Simkovich, N., Farrell, S., Reinagel, P., Bamdad, C., Sigal, G., and Ptashne, M. (1995) *Cell* **81,** 359–368
41. Wach, A., Brachat, A., Pohlmann, R., and Philippsen, P. (1994) *Yeast* **10,** 1793–1808
42. Gietz, R. D., and Sugino, A. (1988) *Gene* (*Amst.*) **74,** 527–534
43. Kaiser, C., Michaelis, S., and Mitchell, A. (1994) *Methods in Yeast Genetics,* pp. 169–173, Cold Spring Harbor Laboratory Press, Cold Spring Harbor, NY
44. Lindner, P., Bauer, K., Krebber, A., Nieba, L., Kremmer, E., Krebber, C., Honegger, A., Klinger, B., Mocikat, R., and Plückthun, A. (1997) *BioTechniques* **22,** 140–149
45. Escher, D., and Schaffner, W. (1997) *Mol. Gen. Genet.* **256,** 456–461
46. Jung, S., and Plückthun, A. (1997) *Protein Eng.* **10,** 959–966
47. Tewari, D., Goldstein, S. L., Notkins, A. L., and Zhou, P. (1998) *J. Immunol.* **161,** 2642–2647
48. Nieba, L., Honegger, A., Krebber, C., and Plückthun, A. (1997) *Protein Eng.* **10,** 435–444
49. Wendt, H., Baici, A., and Bosshard, H. R. (1994) *J. Am. Chem. Soc.* **116,** 6973–6974
50. Zitzewitz, J. A., Bilsel, O., Luo, J., Jones, B. E., and Matthews, C. R. (1995) *Biochemistry* **34,** 12812–12819
51. Grim, J. E., Siegal, G. P., Alvarez, R. D., and Curiel, D. T. (1998) *Biochem. Biophys. Res. Commun.* **250,** 699–703
52. Berger, C., Piubelli, L., Haditsch, U., and Bosshard, H. R. (1998) *FEBS Lett.* **425,** 14–18
53. O'Shea, E. K., Rutkowski, R., and Kim, P. S. (1989) *Science* **243,** 538–542
54. Cardinale, A., Lener, M., Messina, S., Cattaneo, A., and Biocca, S. (1998) *FEBS Lett.* **439,** 197–202
55. Wetzel, R. (1994) *Trends Biotechnol.* **12,** 193–198
56. Chrunyk, B. A., and Wetzel, R. (1993) *Protein Eng.* **6,** 733–738